

## Calcium influx factor is synthesized by yeast and mammalian cells depleted of organellar calcium stores

PETER CSUTORA\*, ZHENGCHANG SU†, HAK YONG KIM‡, ANDREJ BUGRIM§, KYLE W. CUNNINGHAM¶, RICHARD NUCCITELLI||, JOEL E. KEIZER§, MICHAEL R. HANLEY‡, J. EDWIN BLALOCK†, AND RICHARD B. MARCHASE\*,\*\*

Departments of \*Cell Biology and †Physiology and Biophysics, University of Alabama, Birmingham, AL 35294-0005; ‡Department of Biological Chemistry, §Institute of Theoretical Dynamics, and ||Department of Molecular and Cellular Biology, University of California, Davis, CA 95616; and ¶Department of Biology, The Johns Hopkins University, Baltimore, MD 21218

Communicated by Roger Y. Tsien, University of California, San Diego, La Jolla, CA, November 17, 1998 (received for review August 13, 1998)

**ABSTRACT** Depletion of endoplasmic reticulum  $\text{Ca}^{2+}$  stores leads to the entry of extracellular  $\text{Ca}^{2+}$  into the cytoplasm, a process termed capacitative or store-operated  $\text{Ca}^{2+}$  entry. Partially purified extracts were prepared from the human Jurkat T lymphocyte cell line and yeast in which  $\text{Ca}^{2+}$  stores were depleted by chemical and genetic means, respectively. After microinjection into *Xenopus laevis* oocytes, the extracts elicited a wave of increased cytoplasmic free  $\text{Ca}^{2+}$  ( $[\text{Ca}^{2+}]_i$ ) that spread from the point of injection across the oocyte. Extracts from cells with replete organellar  $\text{Ca}^{2+}$  stores were inactive. The increases depended on extracellular  $\text{Ca}^{2+}$ , were unaffected by the inositol 1,4,5-trisphosphate ( $\text{IP}_3$ ) inhibitor heparin or an anti- $\text{IP}_3$  receptor antibody and were unchanged when the endoplasmic reticulum was segregated to the hemisphere opposite the injection site by centrifugation. Confocal microscopy revealed that  $[\text{Ca}^{2+}]_i$  increases were most pronounced at the periphery of the oocyte. The patterns of  $[\text{Ca}^{2+}]_i$  increases were replicated by computer simulations based on a diffusible messenger of about 700 Da that directly activates  $\text{Ca}^{2+}$  influx. In addition,  $I_{\text{CRAC}}$ , a  $\text{Ca}^{2+}$  release-activated  $\text{Ca}^{2+}$  current monitored in Jurkat cells by whole-cell patch clamp recordings, was more rapidly activated when active extracts were included in the patch pipette than by the inclusion of a  $\text{Ca}^{2+}$  chelator or  $\text{IP}_3$ . These data support the existence in yeast and mammalian cells depleted of  $\text{Ca}^{2+}$  stores of a functionally conserved diffusible calcium influx factor that directly activates  $\text{Ca}^{2+}$  influx.

Numerous signal transduction pathways depend on agonist-induced increases in cytoplasmic free  $\text{Ca}^{2+}$  ( $[\text{Ca}^{2+}]_i$ ). The initial phase of this response is often caused by the generation of inositol 1,4,5-trisphosphate ( $\text{IP}_3$ ) and a subsequent release of  $\text{Ca}^{2+}$  from the endoplasmic reticulum (ER). This depletion of ER  $\text{Ca}^{2+}$  stores is generally followed by an influx of extracellular  $\text{Ca}^{2+}$  into the cytoplasm (1), a process termed capacitative (2) or store-operated (3)  $\text{Ca}^{2+}$  entry. This second phase of  $\text{Ca}^{2+}$  mobilization is required for refilling intracellular stores and for cellular responses that depend on a sustained increase in  $[\text{Ca}^{2+}]_i$ , such as the transcriptional regulation in T cells of interleukin-2 (4).

The signal transduction cascade that leads to the opening of the plasma membrane  $\text{Ca}^{2+}$  channels responsible for the capacitative influx appears to be triggered by the emptying of ER  $\text{Ca}^{2+}$  stores and can be activated in the absence of  $\text{IP}_3$  (1). However, neither the plasma membrane channels responsible for  $\text{Ca}^{2+}$  influx (5–7) nor the nature of the signal that conveys the message of ER  $\text{Ca}^{2+}$  depletion to these channels (1, 8) has

been definitively established. Two hypotheses have been put forward to explain this signaling. One argues that a physical association between the ER and the plasma membrane may be involved (9), whereas the other invokes a diffusible messenger (1, 7).

The initial report of one such diffusible messenger, termed Calcium Influx Factor (CIF) by Randriamampita and Tsien (10), demonstrated that an extract from Jurkat cells pretreated with thapsigargin, a selective inhibitor of the ER  $\text{Ca}^{2+}$ -ATPase (11), was able to generate store-operated  $\text{Ca}^{2+}$  entry when applied to a second cell that had previously not been activated. However, the mechanism responsible for the  $\text{Ca}^{2+}$  influx remained unresolved (12). Hanley and colleagues (13–15) demonstrated that a variant of this preparation contained a factor that only when microinjected is able to elicit  $\text{Ca}^{2+}$ -dependent  $\text{Cl}^-$  currents in the plasma membranes of *Xenopus* oocytes or other reporter cells.

The data presented here provide further evidence supporting the existence of a diffusible CIF and contribute to an understanding of this molecule's action in several ways. First, we document the topographic pattern of  $\text{Ca}^{2+}$  increases elicited by CIF in *Xenopus* oocytes using  $\text{Ca}^{2+}$ -sensitive dyes. The progression across the oocyte is consistent with diffusion of a 700-Da messenger and can be modeled by a simulation in which the only function of the diffusible messenger is to activate cell-surface  $\text{Ca}^{2+}$  channels. Second, we demonstrate that the influx pattern is unaffected by a redistribution of the oocyte's ER and distinct from that caused by  $\text{IP}_3$ . Third, we document that yeast genetically depleted of organellar  $\text{Ca}^{2+}$  produce a CIF that elicits  $\text{Ca}^{2+}$  influx in *Xenopus* oocytes and is functionally indistinguishable from that synthesized by mammalian cells. Lastly, we demonstrate using patch-clamp approaches in the Jurkat cell line that yeast CIF activates plasma membrane channels responsible for a previously described  $I_{\text{CRAC}}$  (16).

### MATERIALS AND METHODS

Acid extracts were prepared from thapsigargin-treated and untreated Jurkat cells as described (14). Briefly,  $1.5 \times 10^7$  cells were washed three times and resuspended in Hanks' Balanced Salt Solution containing 20 mM Hepes, pH 7.2. Stimulation was carried out by using 1  $\mu\text{M}$  thapsigargin for 15 min at room temperature. The cells were washed and resuspended in 0.85 ml of Hanks' Balanced Salt Solution. The suspension was extracted with 0.15 ml of 1 M HCl for 30 min at room

The publication costs of this article were defrayed in part by page charge payment. This article must therefore be hereby marked "advertisement" in accordance with 18 U.S.C. §1734 solely to indicate this fact.

© 1999 by The National Academy of Sciences 0027-8424/99/96121-6\$2.00/0  
PNAS is available online at www.pnas.org.

Abbreviations:  $[\text{Ca}^{2+}]_i$ , cytoplasmic free  $\text{Ca}^{2+}$ ; CIF, Calcium Influx Factor; ER, endoplasmic reticulum;  $\text{IP}_3$ , inositol 1,4,5-trisphosphate; NAADP, nicotinic acid adenine dinucleotide phosphate.

\*\*To whom reprint requests should be addressed at: Department of Cell Biology, McCallum Building 690, The University of Alabama at Birmingham, Birmingham, AL 35294-0005. e-mail: marchase@uab.edu.

temperature. After centrifugation, the supernatant was neutralized with 10 M NaOH, and 10 mM BaCl<sub>2</sub> was added to precipitate compounds containing vicinal phosphates including IP<sub>3</sub> (14). After centrifugation, the supernatant was lyophilized and the residue extracted with 0.8 ml methanol with continuous mixing for 20 min. The methanol extract was loaded on a Sep-Pak Vac C18 cartridge, and the cartridge was washed with 0.8 ml methanol. The combined methanol eluates were dried at 30°C under N<sub>2</sub> gas and resuspended in 50 μl of 0.1 M acetic acid. The reconstituted extract was clarified by centrifugal ultrafiltration through a Microcon-30 filter (Amicon). Comparisons between thapsigargin-treated and control cell extracts as assessed by the *Xenopus* oocyte bioassay and all other data shown were routinely performed at this point in the purification. However, most preparations were subjected to Biogel P-2 chromatography (see ref. 14) and anion exchange HPLC liquid chromatography (the activity eluted from a Partisil 10 SAX column as a single peak 25% through a linear salt and pH gradient from 5 to 750 mM (NH<sub>4</sub>)<sub>2</sub>PO<sub>4</sub> and from pH 2.8 to 3.7, respectively). These protocols resulted in a 600-fold enrichment in activity relative to A<sub>259</sub> in the active fractions. The characteristics of the activity were unchanged, and no masked activity was revealed in the control preparations (data not shown).

The same protocol was used to prepare extracts from wild-type (YR98: MAT $\alpha$  *ade2 his3-Δ200 leu2-3, 112 lys2-Δ201 ura3-52*) and *pmr1* (YR122: MAT $\alpha$  *ade2 his3-Δ200 leu2-3, 112 lys2-Δ201 pmr1-Δ1::LEU2 ura3-52*) yeast cells. Yeast cells (30 ml) grown to an OD<sub>600</sub> of 1.5 in yeast extract/peptone/dextrose media were conveniently extracted by using the same volumes of chemicals.

Stage V and VI oocytes were harvested from wild-type and albino *Xenopus laevis*. After defolliculation in 2 mg/ml collagenase, they were injected with 14 nl of 5 mM Fura-2 free acid (Molecular Probes). After 30 min, the oocytes in some experiments were transferred to a centrifuge tube containing 5 ml 30% Ficoll 400. Stratification was carried out at 4,000 × g for 1 hr (17). The oocytes were oriented on the microscope stage with the animal pole facing the objective or, for those that were centrifuged, so that all four layers of the stratified oocyte were visible in the optical plane.

Changes in [Ca<sup>2+</sup>]<sub>i</sub> were measured on an Olympus IX70 inverted microscope (Lake Success, NY) through a 10× UplanAPO objective, numerical aperture = 0.17, equipped with a rapid excitation filter changer alternating between 340 and 380 nm (Ludl Electronics, Hawthorne, NY) and a charge-coupled device camera (Sensys, Photometrics, Tucson, AZ). Changes in fluorescence were analyzed by using the ratio extension of the IP-LAB SPECTRUM imaging software (Signal Analytics, Vienna, VA). Data are expressed relative to the 340/380 nm ratio at *t* = 0. Fura-2 imaging at low magnification in such large relatively pigment-free cells integrates emissions over perhaps 100 microns with [Ca<sup>2+</sup>]<sub>i</sub> responses being more pronounced near the cell periphery (18). For confocal microscopy, albino oocytes were injected with 4 nl of 10 mM Oregon Green Bapta-1 dextran (Molecular Probes). After 30 min, they were transferred to the stage of a Leitz DM IRBE dual laser confocal microscope. Images were collected every 5 sec from 30-μm-thick optical sections by using the Leica (Deerfield, IL) TCS-NT computer system.

Simulations used the OVERTURE software (Los Alamos National Laboratory, Los Alamos, NM), which solved coupled diffusion equations for [CIF] and [Ca<sup>2+</sup>]<sub>i</sub> in a sphere of 1 mm diameter with an axis of symmetry around the line of injection. Equations are:  $\partial X/\partial t = D\nabla^2 X + f$ . For  $X = [\text{CIF}]$ :  $D = 212 \mu\text{m}^2/\text{s}$ ,  $f = 0$  and no flux at the surface; for  $X = [\text{Ca}^{2+}]$ :  $D = 20 \mu\text{m}^2/\text{s}$  and  $f = V_{\text{leak}} - V_{\text{SERCA}} [\text{Ca}^{2+}]^2 / K_{\text{SERCA}}^2 + [\text{Ca}^{2+}]$  [leak from ER - sarcoplasmic/endoplasmic reticulum Ca<sup>2+</sup>ATPase (SERCA) pumping into the ER] and CIF-induced influx =  $k[\text{CIF}]/(K_1 + [\text{CIF}])$  at the surface. The

parameters used: spherical bolus of CIF (radius = 100 μm, centered 300 μm (Fig. 1F) or 100 μm (Fig. 2C) from membrane, amount =  $7.5 \cdot 10^{-7}$  (arbitrary units),  $K_1 = 1.0$  arbitrary units/l,  $V_{\text{leak}} = 0.006 \mu\text{M}/\text{s}$ ,  $V_{\text{SERCA}} = 0.1 \mu\text{M}/\text{s}$ ,  $K_{\text{SERCA}} = 0.4 \mu\text{M}$ ,  $k = 6.3 \cdot 10^{-16} \mu\text{mol}/\text{s} \cdot \mu\text{m}^2$  (Fig. 1E, extracellular [Ca<sup>2+</sup>] = 5 mM) and  $k = 1.26 \cdot 10^{-15} \mu\text{mol}/\text{s} \cdot \mu\text{m}^2$  (Fig. 2C, extracellular [Ca<sup>2+</sup>] = 10 mM). See ref. 19 for formalism.

Conventional whole-cell recording was performed by a List EPC-7 patch clamp amplifier (List Medical Electronic, Darmstadt, Germany). Pipettes were fire polished to produce a tip resistance of 3–5 MΩ. The cytoplasmic-like pipette solution contained 150 mM CsAspartate or CsGlutamate/2 mM MgCl<sub>2</sub>/1 mM CaCl<sub>2</sub>/10 mM CsEGTA (free [Ca<sup>2+</sup>] ≈ 20 nM)/10 mM Hepes, pH 7.2 adjusted with CsOH. The bath solution contained 142 mM NaCl/20 mM CaCl<sub>2</sub>/1 mM MgCl<sub>2</sub>/4.5 mM KCl/10 mM glucose/10 mM Hepes, pH 7.4 adjusted with NaOH. Solution changes in the chamber were achieved by a gravity-feed system and were completed in 1 sec. The capacitive current was compensated, and a tip junction potential of +10 mV was not corrected. For continuous recording of current, cells were held at -40 mV, and the signal was digitized at 20 kHz and recorded on VCR tape. For display, the signal was filtered at 1,000 Hz by an eight-pole low-pass Bessel filter (Model 900, Frequency Devices, Haverhill, MA). A 320-ms voltage ramp from -100 to +100 mV was applied to the cell to obtain current-voltage relationships. In some experiments, the cells were held at 0 mV after whole-cell was achieved, and activation of I<sub>CRAC</sub> was detected by applying a 260-ms voltage step to -80 mV at a frequency of 0.2 Hz. The currents were sampled at 5 kHz and filtered at 1 kHz by the low-pass Bessel filter. The data were analyzed by PCLAMP software (Axon Instruments, Foster City, CA).

## RESULTS

Partially purified acid extracts were prepared from Jurkat cells pretreated with thapsigargin, as previously described (14). To provide topographic information regarding the Ca<sup>2+</sup> influx elicited by such extracts, we assessed [Ca<sup>2+</sup>]<sub>i</sub> responses in albino *Xenopus* oocytes using Fura-2 (20). A time course of the changes in the 340/380-nm fluorescence ratio after injection of a partially purified extract from the thapsigargin-treated cells relative to that at the time of injection is shown as a series of pseudocolored images (Fig. 1A). Increases in [Ca<sup>2+</sup>]<sub>i</sub> were seen near the point of injection within seconds and then spread across the oocyte. In contrast, acid extracts prepared from untreated cells elicited fluorescence ratio changes less than 5% of those shown (Fig. 1C).

In *Saccharomyces cerevisiae*, depletion of Ca<sup>2+</sup> from secretory pathway organelles is achieved by mutation of the Ca<sup>2+</sup>ATPase encoded by *PMR1* (21) and results in an elevated uptake of extracellular calcium (22). Reasoning that a functional response to store depletion might be evolutionarily conserved, extracts were prepared (14) from *pmr1* mutants. These also elicited robust increases in oocyte [Ca<sup>2+</sup>]<sub>i</sub> that again were initiated near the point of injection and then moved across the oocyte (Fig. 1B). We found that oocyte responses depended on the *pmr1* extract's concentration. The half-maximal value corresponded to an injection of 35,000 cell equivalents (Fig. 1D). Extracts prepared from wild-type yeast were not active (Fig. 1C). Application of cell extracts to the exterior of oocytes failed to trigger Ca<sup>2+</sup> influx (Fig. 1C), suggesting that the putative CIFs are membrane impermeable and act independently of cell-surface receptors that might trigger donor cell store depletion and subsequent Ca<sup>2+</sup> influx.

A related issue is whether the primary activity of the intracellularly active substance is to stimulate Ca<sup>2+</sup> influx at the oocyte plasma membrane or, like IP<sub>3</sub>, to elicit release from intracellular Ca<sup>2+</sup> stores within the oocyte, which then triggers

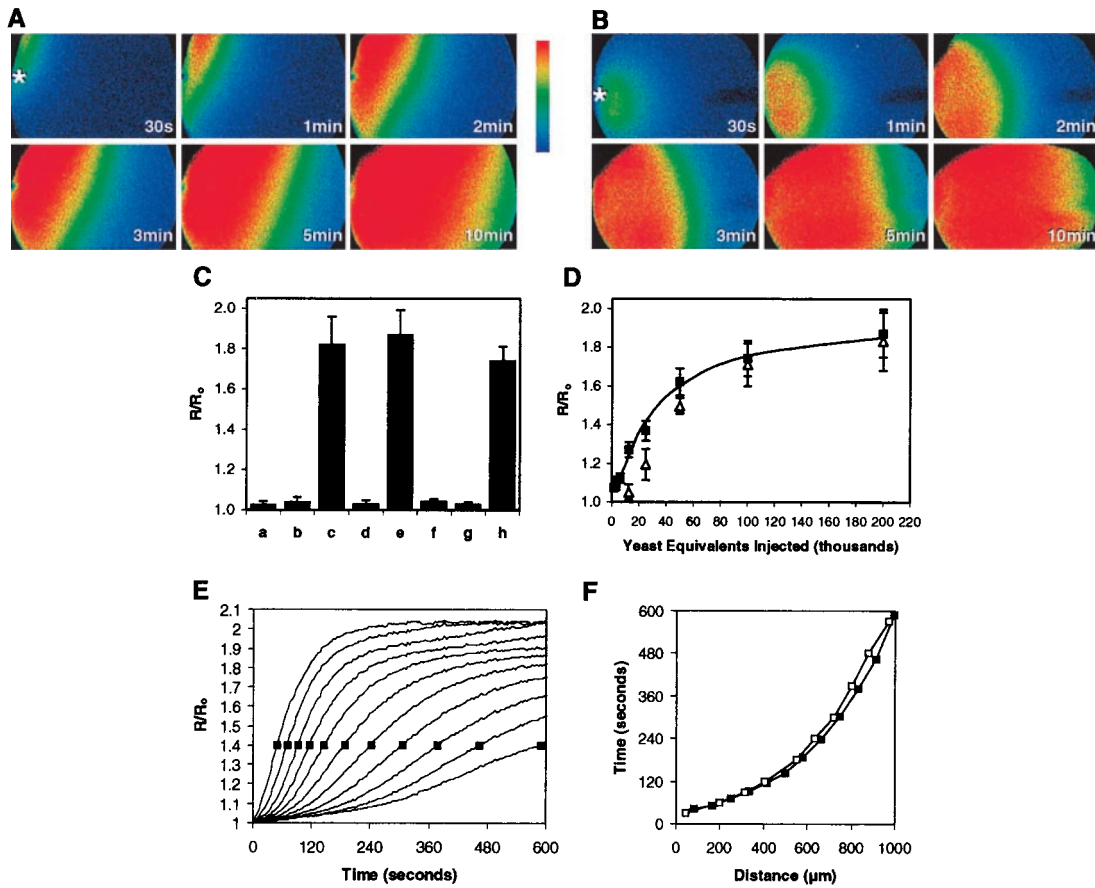


FIG. 1. (A) Pseudocolored ratiometric images of an albino *Xenopus* oocyte preloaded with Fura-2 after injection at  $t = 0$  of 14 nl of acid extract prepared from the equivalent of 5,000 thapsigargin-treated Jurkat cells. Increases in the 340/380 nm ratio relative to those at the time of injection are shown. Extracellular  $Ca^{2+}$  was 5 mM. The asterisk in the first frame denotes the point of injection. Data shown are representative of injections of 15 independent preparations. (B) Pseudocolored images after injection of an acid extract corresponding to approximately 200,000 *pmr1* yeast cells. Data shown are representative of injections of 25 independent preparations. (C) Increases in fluorescence ratio for extracts prepared from: (a) untreated Jurkat cells; (b) Jurkat cells in which thapsigargin was added immediately before acid extraction; (c) Jurkat cells extracted 15 min after thapsigargin treatment; (d) wild-type yeast; (e) *pmr1* yeast; (f) *pmr1* yeast, but the oocytes were bathed in a medium containing 5 mM EGTA; (g) *pmr1* yeast, but the extract was applied extracellularly; (h) *pmr1* yeast, but the extract was coinjected with heparin (3,000 Da) at a final cytoplasmic concentration estimated to be 200  $\mu$ M. The data are means of from 3 to 10 replicates. Standard deviations are shown. (D) Increases in fluorescence as a function of increasing concentrations of the yeast extract in the absence ( $\blacksquare$ ) and presence ( $\blacktriangle$ ) of 2 mM  $LaCl_3$ . The data in C and D refer to the maximal  $R/R_0$  averaged over a  $500 \times 700\text{-}\mu\text{m}$  area containing  $\approx 45\%$  of the oocyte including the injection site. (E) Time course of ratiometric increases shown in A for a series of 80- $\mu\text{m}$  wide segments spanning the oocyte from the point of injection (leftmost curve) and progressing to the opposite side (rightmost curve). Measurements are from the oocyte's plasma membrane at the point of penetration to the center of each segment. (F) Times to reach a fluorescence ratio of 1.4 (shown as boxes in E) for each of the segments depicted in E. Comparable patterns were detected in multiple independent preparations from Jurkat ( $\blacksquare$ ) and *pmr1* yeast (data not shown). Also shown ( $\square$ ) is the simulated progression of  $[Ca^{2+}]_i$  increases due to a diffusible CIF (19).

an endogenous cascade leading to  $Ca^{2+}$  entry. Two observations are relevant. First, the magnitude of the responses to

thapsigargin and  $IP_3$  are modest ( $R/R_0 < 1.2$ ) compared with the responses seen to the positive preparations. Second, the

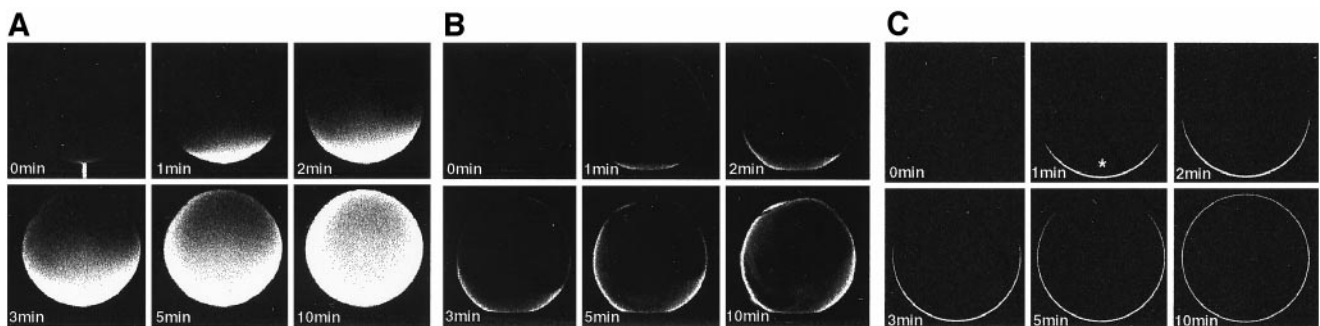


FIG. 2. Dual laser confocal images of a horizontal 30- $\mu\text{m}$  optical plane near the equator of an albino *Xenopus* oocyte preloaded with Oregon Green Bapta-1 dextran. At  $t = 0$  14 nl of acid extract prepared from *pmr1* yeast were injected along with Alexa 594 hydrazide. Extracellular  $Ca^{2+}$  was 10 mM. (A) Time course of Alexa 594 fluorescence. At  $t = 0$  the dye is visible in the pipette ( $n = 4$ ). (B) Time course showing  $[Ca^{2+}]_i$  as assessed by fluorescence of Oregon Green Bapta-1 dextran ( $n = 5$ ). (C) Simulation of a confocal image modeling  $[Ca^{2+}]_i$  increases from 150 to 300 nM after an injection of CIF (14). The asterisk denotes the site of the injection.

influx caused by IP<sub>3</sub> or thapsigargin is effectively blocked by lanthanides (23, 24). Whereas the modest [Ca<sup>2+</sup>]<sub>i</sub> responses to low levels of the putative CIFs are up to 75% inhibited by La<sup>3+</sup>, the more robust responses to higher concentrations are to a large extent resistant to lanthanides (Fig. 1D).

Other results also argue against an IP<sub>3</sub>-like release from stores. First, the increase in [Ca<sup>2+</sup>]<sub>i</sub> elicited by these extracts from thapsigargin-treated Jurkat cells and *pmr1* yeast was completely lacking when Ca<sup>2+</sup> in the oocyte bath was chelated (Fig. 1C). Second, coinjection of heparin at levels that block IP<sub>3</sub>-mediated Ca<sup>2+</sup> release from intracellular stores (25) had no effect on Ca<sup>2+</sup> influx evoked by the putative yeast CIF (Fig. 1C). Third, coinjection of 0.3 mg/ml of IG9, a polyclonal antibody to the IP<sub>3</sub> receptor that blocks IP<sub>3</sub>-induced Ca<sup>2+</sup> release in *Xenopus* embryos (26), had no effect on CIF-induced increases (data not shown).

We also determined the time courses for changes in ratio after injection of the Jurkat extract depicted in Fig. 1A in 11 adjacent 80- $\mu$ m segments that span the breadth of the cell (Fig. 1E). The progression of a 40% increase in fluorescence ratio across the segments was highly reproducible, averaging in multiple trials approximately 4  $\mu$ m/sec near the injection site and decreasing to less than 1  $\mu$ m/sec near the opposite pole (Fig. 1F). Next, we constructed a simulation based simply on the three-dimensional diffusion of a small molecule, the only activity of which is to elicit Ca<sup>2+</sup> influx at the plasma membrane. By selecting a diffusion constant appropriate for a  $\approx$ 700-Da CIF, a remarkable correspondence to the experimental data was achieved (Fig. 1F).

In addition, laser confocal microscopy was used to define more precisely the topography and kinetics of [Ca<sup>2+</sup>]<sub>i</sub> increases. In the experiment shown in Fig. 2, the *pmr1* extract was coinjected with a 759-Da fluorescent marker, Alexa 594 hydrazide, into oocytes that had been previously injected with the nonratiometric Ca<sup>2+</sup> indicator Oregon Green Bapta-1 dextran. Alexa 594 was selected for this experiment because its molecular mass is similar to the apparent size of the CIF activity in molecular sieve chromatography (data not shown), although diffusion properties are influenced by other variables as well. Alexa 594 spread from the point of injection evenly across the section at a rate of approximately 2–3  $\mu$ m/sec (Fig. 2A). Increases in [Ca<sup>2+</sup>]<sub>i</sub> (Fig. 2B) also spread from the point of injection but were apparent only along the perimeter of the oocyte. The progression rate of this [Ca<sup>2+</sup>]<sub>i</sub> increase was nearly identical to that seen with Alexa 594. These data are consistent with a model in which the putative CIF diffuses throughout the oocyte in a manner similar to Alexa 594, but in which the influx of Ca<sup>2+</sup> across the plasma membrane triggered by CIF remains restricted to the cortical area because of the poor diffusion characteristics of Ca<sup>2+</sup> in the cytoplasmic environment (19). A simulation of [Ca<sup>2+</sup>]<sub>i</sub> increases based on the model previously described is shown in Fig. 2C, and again a high level of correspondence to our data is seen.

Although not apparent in Fig. 2B, increases in fluorescence in the interior of such sections corresponding to less than 5% of those observed at the periphery were reproducibly detected. These increases did not depend on extracellular Ca<sup>2+</sup> and spread from the point of injection across the sections at a rate comparable to that of Alexa 594. As with the much larger increases seen at the sections' peripheries, this apparent release from intracellular stores was not inhibited by the anti-IP<sub>3</sub> receptor antibody (data not shown). Injections of Ca<sup>2+</sup> (27), IP<sub>3</sub> (18, 28), cyclic ADP ribose (29), and nicotinic acid adenine dinucleotide phosphate (NAADP) (29), even at high concentrations, did not result in [Ca<sup>2+</sup>]<sub>i</sub> increases that resembled those observed with our preparations. In other experiments (data not shown), CIF was injected near the center of the oocyte. Only very modest [Ca<sup>2+</sup>]<sub>i</sub> responses emanating from the oocyte's center were seen for 2–3 min, but then 20-fold

larger increases were seen at nearly the same time all around the oocyte's periphery.

We asked next whether disrupting the topography of the ER would affect our results. We used centrifugation to localize the vast majority of ER to a relatively narrow band (17). Fig. 3A shows a photomicrograph of the centrifuged oocytes, in which [Ca<sup>2+</sup>]<sub>i</sub> increases in response to IP<sub>3</sub> and thapsigargin were previously localized to the portion of the oocyte enriched for the ER (17, 30). Our observations also showed maximal [Ca<sup>2+</sup>]<sub>i</sub> increases near this band and were faithfully mimicked by a model based on a diffusible CIF produced only by the ER-enriched band (A.B., P.C., R.B.M., and J.E.K., manuscript in preparation). The localization of the ER was also confirmed by immunofluorescence using an antibody specific for the ER marker calnexin (Fig. 3B). We determined the effects of injection of the *pmr1* extract on the side of the oocyte opposite

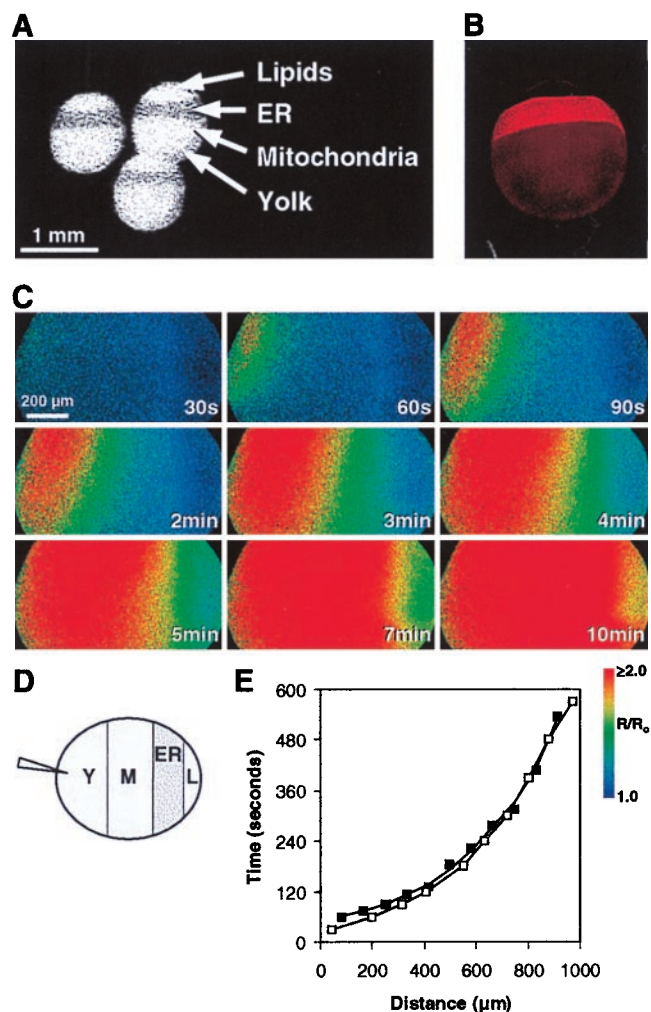


FIG. 3. (A) Photomicrograph of albino *Xenopus* oocytes after centrifugation showing the stratification of its contents. The layers of the stratified oocyte are labeled as described previously (17, 18). (B) Visualization of ER layer in a stratified oocyte. Albino *Xenopus* oocytes were fixed with formaldehyde, permeabilized with absolute methanol, and processed for anti-calnexin immunofluorescence. (C) Pseudocolored images of a stratified oocyte injected at  $t = 0$  with 14 nl of an extract from *pmr1* yeast at a point opposite the ER-enriched band. The images show the ER-enriched band on the right, rotated 90° from the images shown in A and B. Extracellular Ca<sup>2+</sup> was 5 mM. (D) Diagrammatic representation showing the point of injection in C relative to the ER-enriched band. (E) Times to reach a fluorescence ratio of 1.4 for a series of 80- $\mu$ m segments spanning the oocyte (■). Also shown (□) is the simulated progression of [Ca<sup>2+</sup>]<sub>i</sub> increases replicated from Fig. 1F.

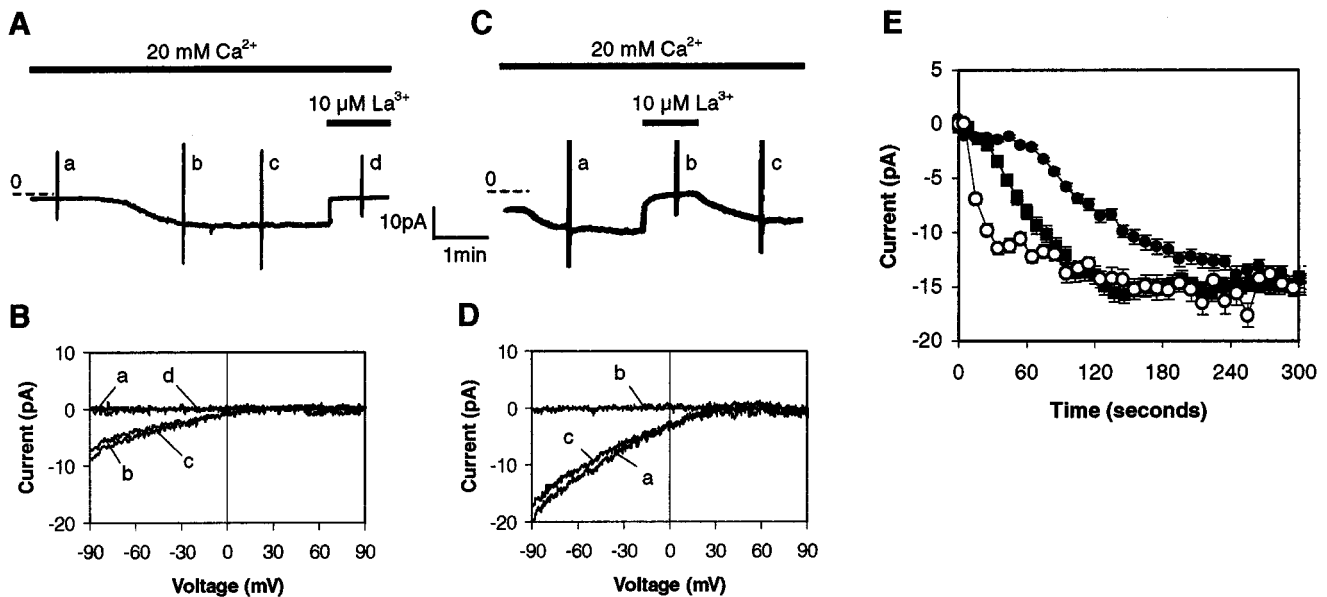


FIG. 4. (A) Time course of  $\text{Ca}^{2+}$  current after achievement of whole-cell configuration with a pipette containing extract prepared from wild-type yeast. The pipette contained  $\approx 300$  yeast equivalents per nl. (B) The current–voltage relationships recorded at the time points labeled *a–d* in A. Voltage ramps ranging from  $-100$  to  $100$  mV were applied. Portions of the capacitive current that are observed at the extremes of the voltage ramps are left as event markers in A and C, but are not shown in B or D. (C) Time course of  $\text{Ca}^{2+}$  current after achievement of whole-cell configuration with a pipette containing extract prepared from *pmr1* yeast. (D) The current–voltage relationships recorded at the time points labeled *a–d* in C. (E) Comparison of the time courses of  $\text{I}_{\text{CRAC}}$  activation by  $10 \mu\text{M}$   $\text{IP}_3$  ( $\blacksquare$ ,  $n = 9$ ), and extracts from wild-type ( $\bullet$ ,  $n = 14$ ) and *pmr1* yeast ( $\circ$ ,  $n = 9$ ). Standard errors are shown.

the ER band (Fig. 3D). Increase in  $[\text{Ca}^{2+}]_i$  that progressed across the breadth of the cell were seen (Fig. 3C) that were indistinguishable from those observed with nonstratified oocytes and from the simulation (Fig. 3E). In other experiments, injections were made at various points around the centrifuged oocyte, including near the ER band. In each case, increase in  $[\text{Ca}^{2+}]_i$  began near the injection site and spread across the oocyte in a manner similar to that depicted above.

To determine whether the putative yeast CIF were effective in mammalian cells and to begin to characterize the responsible  $\text{Ca}^{2+}$  channels, we performed whole-cell patch clamp recordings of Jurkat T cells. When the pipette solution contained the  $\text{Ca}^{2+}$  chelator EGTA, with or without wild-type yeast extract ( $n = 28$ ), a slowly activated  $\text{Ca}^{2+}$  current was observed that required, on the average, about 200 sec to fully activate after achievement of the whole-cell configuration (Fig. 4A). Such a current has been described previously with  $\text{Ca}^{2+}$  chelators present in the pipette (16), and the presence of the wild-type yeast extract had no effect on the kinetics of activation. This current could be completely blocked by  $10 \mu\text{M}$   $\text{La}^{3+}$  (Fig. 4A). It was inwardly rectified with a reversal potential near  $+60$  mV (Fig. 4B), was less permeable to  $\text{Ba}^{2+}$  than  $\text{Ca}^{2+}$ , had a 1,000-fold selectivity for  $\text{Ca}^{2+}$  over  $\text{Na}^+$  but became permeable to monovalent cations in the absence of divalents (data not shown). These characteristics are consistent with those of the previously described  $\text{I}_{\text{CRAC}}$  (16). In contrast, when the pipette solution contained *pmr1* yeast extract (Fig. 4C), a  $\text{Ca}^{2+}$  current was much more rapidly activated ( $n = 30$ ). All characteristics of the CIF-induced current were consistent with its identification as  $\text{I}_{\text{CRAC}}$  (Fig. 4D and data not shown). Virtually identical results were seen with CIF preparations from thapsigargin-treated Jurkat cells (data not shown).

We quantitated the time courses of the activation of  $\text{I}_{\text{CRAC}}$  by dialysis of the cytosol with either wild-type or *pmr1* yeast extracts or with  $\text{IP}_3$ . The times to achieve an  $\text{I}_{\text{CRAC}}$  of 7.5 pA in Jurkat T cells by wild-type yeast extracts and  $10 \mu\text{M}$   $\text{IP}_3$  were 120 and 56 sec, respectively (Fig. 4E). In contrast, the activation of  $\text{I}_{\text{CRAC}}$  induced by *pmr1* extracts was much more rapid, reaching 7.5 pA by 17 sec. Although the time constant of

activation with  $\text{IP}_3$  depends on  $[\text{IP}_3]$  (31), even at  $50 \mu\text{M}$   $\text{IP}_3$  activation with CIF was at least as rapid (data not shown). The nearly immediate activation of  $\text{I}_{\text{CRAC}}$  by *pmr1* yeast extracts is consistent with a model in which CIF is active in the signaling cascade at a step downstream of  $\text{IP}_3$ .

## DISCUSSION

These data demonstrate that a CIF prepared from either mammalian or yeast cells depleted of ER/Golgi  $\text{Ca}^{2+}$  elicits  $\text{Ca}^{2+}$  influx across the plasma membranes of two different indicator cells. Furthermore, extracts from cells with normal levels of sequestered  $\text{Ca}^{2+}$  were devoid of CIF activity. Since a CIF activity was first described (10), its mode of action and other characteristics have remained controversial (12). Collectively, the data presented here provide substantial new support for the existence of such a signaling molecule.

Although a modest increase in  $[\text{Ca}^{2+}]_i$  is elicited in oocytes by our preparations independent of influx, there is substantial evidence that a direct activation of  $\text{Ca}^{2+}$  entry is primarily responsible for the increases in  $[\text{Ca}^{2+}]_i$  we observe. First, activation of an influx of comparable magnitude could not be achieved by  $\text{Ca}^{2+}$ , thapsigargin,  $\text{IP}_3$ , cyclic ADP ribose, or NAADP, all of which are effective in various contexts at releasing sequestered  $\text{Ca}^{2+}$ . In addition, the influx we observed at high concentrations of our preparations was resistant to inhibition by lanthanides, in contrast to influx caused by  $\text{IP}_3$  or thapsigargin (23, 24). The probability of an  $\text{IP}_3$ -like contaminant is further decreased by the lack of effect of heparin or an  $\text{IP}_3$  activity-blocking antibody. Second, redistribution of the vast majority of the ER by centrifugation has no effect on the activation. Third, the wave of  $[\text{Ca}^{2+}]_i$  increases induced by our preparations is distinct from any previously observed in oocytes and is faithfully mimicked by the simulation with a direct activator of influx. Fourth, when  $\text{IP}_3$  is used to empty the intracellular  $\text{Ca}^{2+}$  stores in mature oocytes, the increases in  $[\text{Ca}^{2+}]_i$  seen in the interior of the oocytes in confocal sections are much larger than those at the cell periphery dependent on extracellular  $\text{Ca}^{2+}$  (32). In contrast, the  $[\text{Ca}^{2+}]_i$  increases we

observe are more than 20 times larger at the cell surface than those in the interior. Fifth, the latency before activation of  $I_{CRAC}$  in mammalian cells is less than that seen with  $IP_3$  or other agents that first release  $Ca^{2+}$  from stores. Together, these data are most consistent with a CIF primarily acting directly at the plasma membrane.

We were surprised that the  $Ca^{2+}$  influx activated by the putative CIFs was not identical to the influx stimulated when the oocytes'  $Ca^{2+}$  stores are depleted (23, 24). This latter influx is sensitive to lanthanides and smaller in magnitude than the maximal response we observed. Auld *et al.* (23) found three distinct  $Ca^{2+}$  influx pathways in oocytes. Only one of those was activated by store depletion, and it was inhibited by lanthanides. A second channel, activated by guanosine 5'-[thio]triphosphate, was insensitive to lanthanides and had a 15-fold higher initial rate of  $Ca^{2+}$ -mediated fluorescence increase. The most parsimonious explanation of our data is that oocyte store depletion produces relatively low levels of CIF, a supposition supported by CIF preparations from these cells (M.R.H., unpublished observation). This level of CIF activates the store-operated  $Ca^{2+}$  channel, consistent with our data that show a 75% block by lanthanides at low CIF concentrations (Fig. 1D). At higher levels of CIF, an additional, higher-capacity lanthanide-insensitive channel is also activated. This channel is responsible for the bulk of the response we observe. A similar breadth of action is seen in mammalian cells, as CIF is able to activate both  $I_{CRAC}$  and a less selective  $Ca^{2+}$  influx channel in Jurkat cells (manuscript in preparation, Z.S., P.C., R.B.M., and J.E.B.).

One intriguing aspect of the  $[Ca^{2+}]_i$  increases we observed in oocytes is that they are relatively long-lasting in the oocyte cytoplasmic environment. In experiments not shown,  $[Ca^{2+}]_i$  was monitored for longer periods of time. Significant decreases in the fluorescence ratio became apparent only after 30 min. These data are similar to the persistence of  $Ca^{2+}$  influx-dependent  $Cl^-$  currents seen by DeLisle *et al.* in these cells after injection of a large amount of  $IP_3$  (28). They may reflect the relative absence of catabolic processes in this cell that in mammalian cells lead to more rapid inactivation of the influx (7). It is also worth noting that the 5,000 Jurkat cell or 200,000 yeast cell equivalents required for full activation in oocytes each correspond to a cytoplasmic volume of approximately 5 nl. Thus, assuming full recovery, the total oocyte cytoplasmic volume is greater by a factor of about 100 than the donor cytoplasm. This comparison suggests that cells with severely depleted  $Ca^{2+}$  stores make far more CIF than is required for activation.

The finding that yeast that are unable to sequester  $Ca^{2+}$  in organelles of the secretory pathway make a putative CIF suggests that the mechanism for repletion of depleted  $Ca^{2+}$  stores is functionally conserved across a broad expanse of evolution. This finding also eliminates the possibility that thapsigargin is necessary for the CIF response, since a genetic rather than chemical effect on an organellar  $Ca^{2+}$ ATPase is responsible for store depletion. Although complete characterization of a CIF from any source has not yet been achieved, putative CIFs from both vertebrate and invertebrate animal cells as well as yeast share all biological, physical, and chemical characteristics assessed to date (unpublished observations), consistent with the possibility of structural conservation as well. Such conservation would appear to underscore the fundamental nature of  $Ca^{2+}$  as a signaling molecule and the

importance of providing a mechanism for maintaining its intracellular stores.

We thank Michael Quick for his expertise and assistance with the oocyte isolation, Albert Tousson for his contribution to the immunofluorescence micrograph, Ray Fontanilla for his help with confocal microscopy, and Sherry Crittenden for expert secretarial assistance. We also thank Timothy Walseth for providing cyclic ADP ribose and NAADP. This work was supported by the Fifty 50 Food Juvenile Diabetes Foundation International Program Project Grant (R.B.M.), the Searle Scholars Program/The Chicago Community Trust (K.W.C.), and research grants from the National Institutes of Health (MH52527, J.E.B.; RR10081, J.E.K.; GM53082, K.W.C.; HD19966, R.N.).

1. Thomas, D., Kim, H. Y. & Hanley, M. R. (1998) *Vitam. Horm.* **54**, 97–119.
2. Putney, J. W. & Bird, G. S. J. (1993) *Cell* **75**, 199–201.
3. Clapham, D. E. (1995) *Cell* **80**, 259–268.
4. Rao, A., Luo, C. & Hogan, P. G. (1997) *Ann. Rev. Immunol.* **15**, 707–747.
5. Clapham, D. E. (1996) *Neuron* **16**, 1069–1072.
6. Birnbaumer, L., Zhu, X., Jiang, M., Boulay, G., Peyton, M., Vannier, B., Brown, D., Platano, D., Sadeghi, H., Stefani, E., *et al.* (1996) *Proc. Natl. Acad. Sci. USA* **93**, 15195–15202.
7. Parekh, A. B. & Penner, R. (1997) *Physiol. Rev.* **77**, 901–930.
8. Berridge, M. J. (1995) *Biochem. J.* **312**, 1–11.
9. Petersen, C. C. H. & Berridge, M. J. (1996) *Eur. J. Physiol.* **432**, 286–292.
10. Randriamampita, C. & Tsien, R. Y. (1993) *Nature (London)* **364**, 809–818.
11. Thastrup, O., Cullen, P. J., Drobak, B. K., Hanley, M. R. & Dawson, A. P. (1990) *Proc. Natl. Acad. Sci. USA* **87**, 2466–2470.
12. Gilon, P., Bird, G. J., Bian, X., Yakel, J. L. & Putney, J. W., Jr. (1995) *J. Biol. Chem.* **270**, 8050–8055.
13. Kim, H. Y., Thomas, D. & Hanley, M. R. (1995) *J. Biol. Chem.* **270**, 9706–9708.
14. Thomas, D. & Hanley, M. R. (1995) *J. Biol. Chem.* **270**, 6429–6432.
15. Thomas, D., Kim, H. Y. & Hanley, M. R. (1996) *Biochem. J.* **318**, 649–656.
16. Hoth, M. & Penner, R. (1992) *Nature (London)* **355**, 353–356.
17. Han, J.-K. & Nuccitelli, R. (1990) *J. Cell Biol.* **110**, 1103–1110.
18. Larabell, C. & Nuccitelli, R. (1992) *Dev. Biol.* **153**, 347–355.
19. Jafri, M. S. & Keizer, J. (1995) *Biophys. J.* **69**, 2139–2153.
20. Gryniewicz, G., Poenie, M. & Tsien, R. Y. (1985) *J. Biol. Chem.* **260**, 3440–3450.
21. Rudolph, H. K., Antebi, A., Fink, G. R., Buckley, C. M., Dorman, T. E., LeVitre, J., Davidow, L. S., Mao, J. I. & Moir, D. T. (1989) *Cell* **58**, 133–145.
22. Halachmi, D. & Eilam, Y. (1996) *FEBS Lett.* **392**, 194–200.
23. Auld, A. M., Bawden, M. J., Berven, L. A., Harland, L., Hughes, B. P. & Barritt, G. J. (1996) *Cell Calcium* **19**, 439–452.
24. Yao, Y. & Tsien, R. Y. (1997) *J. Gen. Physiol.* **109**, 703–715.
25. Nuccitelli, R., Yim, D. L. & Smart, T. (1993) *Dev. Biol.* **158**, 200–212.
26. Kume, S., Muto, A., Inoue, T., Suga, K., Okano, H. & Mikoshiba, K. (1997) *Science* **278**, 1940–1943.
27. DeLisle, S. & Welsh, M. J. (1992) *J. Biol. Chem.* **267**, 7963–7966.
28. DeLisle, S., Blondel, O., Longo, F. J., Schnabel, W. E., Bell, G. I. & Welsh, M. J. (1996) *Am. J. Physiol.* **270**, C1255–C1261.
29. Lee, H. C. (1997) *Physiol. Rev.* **77**, 1133–1164.
30. Jaconi, M., Pyle, J., Bortolon, R., Ou, J. & Clapham, D. (1997) *Curr. Biol.* **7**, 599–602.
31. Huang, Y. & Putney, J. W. (1998) *J. Biol. Chem.* **273**, 19554–19559.
32. Fontanilla, R. A. & Nuccitelli, R. (1998) *Biophys. J.* **75**, 2079–2087.